Introduction

Drought has significant direct and indirect impacts on forest health. In direct terms, low-to-moderate drought stress limits plant growth, while more severe drought stress reduces both growth and photosynthetic activity (Kareiva and others 1993, Mattson and Haack 1987). Indirectly, drought stress in forest communities may predispose trees to insect infestation, in some cases leading to major outbreaks (Mattson and Haack 1987). In addition, drought slows organic matter decomposition and reduces the moisture content of woody debris and other fuels, greatly increasing fire risk in wildland areas (Clark 1989, Keetch and Byram 1968, Schoennagel and others 2004).

Several indices have been developed for regional drought monitoring. The most commonly used of these indices is the Palmer Drought Severity Index (PDSI), which is derived from data on total precipitation, precipitation periodicity, and soil characteristics related to moisture supply (Heim 2002). Despite its continued popularity, the PDSI has been criticized for many reasons, including the complexity of its calculation and a lack of spatial comparability between regions of the United States and across different time periods (Alley 1984, Guttman 1998). Moreover, the PDSI is considered an index of meteorological drought,

as is the more recently derived Standardized Precipitation Index (SPI); other indices, some related to the PDSI, have been developed to instead target hydrological drought, e.g., Palmer Hydrologic Drought Severity Index, or agricultural drought, e.g., the Crop Moisture Index and the Palmer Z-Index (Keyantash and Dracup 2002).

The National Climatic Data Center (NCDC) calculates the PDSI monthly for each climate division in the conterminous United States, and provides PDSI data for every month from 1895 to present through a publicly accessible archive (National Climatic Data Center 2007). The U.S. Drought Monitor project, a collaborative effort of the National Drought Mitigation Center, the U.S. Department of Agriculture, and the National Oceanic and Atmospheric Administration, produces weekly contour maps utilizing a blend of drought indices, including the PDSI, as well as daily streamflow percentiles and a remotely sensed vegetation health index (Svoboda and others 2002). These maps may be downloaded in Geographic Information System (GIS) format (National Drought Mitigation Center 2008). Although the PDSI data available through the NCDC archive and the U.S. Drought Monitor maps may serve as adequate reference for broadscale summaries, they are not well suited for analyses involving finer scale covariates or response variables. Because these and other

CRITERION 3—

Chapter 4. High-Resolution Mapping of Drought Conditions

Frank H. Koch[1]

John W. Coulston

William D. Smith

45

[1] Corresponding author: Frank H. Koch, Research Ecologist, U.S. Department of Agriculture Forest Service, Southern Research Station, Research Triangle Park, NC 27709 (formerly Research Assistant Professor, North Carolina State University, Department of Forestry and Environmental Resources, Raleigh, NC 27695).

similar drought monitoring tools are typically derived from point-based weather station data, they have limited spatial precision and are regionally variable in terms of spatial accuracy and detail (Brown and others 2008). Therefore, we adopted a primary objective of developing a methodology for mapping drought stress using historical, high-spatial-resolution climate data that provides complete coverage of the conterminous United States. We wanted our methodology to be computationally simple and require only limited inputs, yet still allow for reasonable comparison of moisture conditions between different geographic areas and time periods.

Methods

We used gridded data (approximately 4-km^2 spatial resolution) created with the Parameter-Elevation Regression on Independent Slopes (PRISM) climate mapping system to complete our analyses. The PRISM system is knowledge based, integrating a localized climate-elevation regression function with other algorithmic components: topographic facets; coastal proximity; a two-layer atmosphere, i.e., a boundary layer and the free atmosphere above it; and weighting of weather station observations based on these and other factors (Daly and

others 2002). At the time we performed our analyses, grids depicting total precipitation, mean daily minimum temperature, and mean daily maximum temperature for the conterminous United States were available monthly from 1895 to 2007 (although the December 2007 grids were preliminary rather than final datasets). All data were available for public download from the PRISM group Web site (PRISM Group 2008).

Calculating a Moisture Index— We adopted an approach, utilizing the PRISM climate grids, in which a moisture index value for a given location, i.e., a grid cell, is calculated based on both precipitation and potential evapotranspiration values for that location during the time period of interest. Potential evapotranspiration measures the loss of soil moisture through plant uptake and transpiration (Akin 1991). It does not measure actual moisture loss, but rather the loss that would occur under ideal conditions, i.e., if there were no possible shortage of moisture for plants to transpire (Akin 1991, Thornthwaite 1948). The inclusion of both precipitation and potential evapotranspiration provides a fuller accounting of the water balance of a location than precipitation alone. So, to complement the PRISM monthly precipitation grids, we

computed monthly potential evapotranspiration grids using the Thornthwaite formula (Akin 1991, Thornthwaite 1948):

$$PET_m = 1.6L(10\frac{T_m}{I})^a \qquad (1)$$

where

PET_m = the potential evapotranspiration for a given month m in cm

L = a correction factor for the hours of daylight and number of days in a month for all locations at a particular latitude

T_m = the mean temperature for month m in degrees C

I = an annual heat index, calculated as $I = \sum_{i=1}^{12} \left(\frac{T_i}{5}\right)^{1.514}$, where T_i is the mean temperature for each month i of the year

a = an arbitrary exponent calculated by $a = 6.75 \times 10^{-7}I^3 - 7.71 \times 10^{-5}I^2 + 1.792 \times 10^{-2}I + 0.49239$

To implement equation 1 spatially, we created a grid of latitude values for determining the L adjustment for any given 4-km^2 grid cell in the conterminous United States [see Thornthwaite (1948) for a table of L correction factors]. We calculated the mean

monthly temperature grids as the mean of the corresponding PRISM daily minimum and maximum monthly temperature grids.

Thornthwaite also proposed an equation for calculating a moisture index based on precipitation and potential evapotranspiration (Akin 1991):

$$MI = 100\frac{P - PET}{PET}$$

where

MI = moisture index

P = precipitation

PET = potential evapotranspiration

(P and PET must be in equivalent measurement units, e.g., mm)

Thornthwaite's MI can be calculated for any time period of interest by totaling precipitation and potential evapotranspiration during the period and entering these two quantities into the equation. It has a lower bound of -100, but does not have an upper bound; if precipitation during the time period is very high and/or potential evapotranspiration is very low, the index value can be over 100. Willmott and Feddema (1992) argued that a better index would be bounded meaningfully at both ends of the scale and

would also be symmetric around zero. They proposed a modified version of Thornthwaite's index with the following form:

$$MI' = \begin{cases} P/PET - 1 & , \quad P < PET \\ 1 - PET/P & , \quad P \geq PET \\ 0 & , \quad P = PET = 0 \end{cases}$$

This set of equations yields a dimensionless index scaled between −1 and 1. As with Thornthwaite's formulation, MI' can be calculated for any time period but is typically calculated on an annual basis (Willmott and Feddema 1992). An alternative to the annual summation approach, which we adopted for these analyses, is to calculate MI' from monthly precipitation and potential evapotranspiration values and then, for a given year, calculate the annual MI' as the mean of the 12 monthly MI' values. This "mean-of-months" approach limits the ability of short-term peaks in either precipitation or potential evapotranspiration to negate corresponding short-term deficits, as would happen under an annual summation approach.

100-Year Normal Moisture Index Map— Applying the modified equations of Willmott and Feddema (1992) to the gridded precipitation and potential evapotranspiration data, we calculated annual MI' grid maps for each year from 1907 to 2006. We then calculated a normal annual MI' grid as the mean of these 100 MI' grids. Although we also calculated a 2007 MI' grid, we did not include it in this normal calculation because the December 2007 PRISM data were preliminary at the time of analysis.

Drought Category Thresholds and Probabilities Based on Moisture Index Difference—We calculated moisture index difference (MID) grids for each year, including 2007, by subtracting the 100-year normal annual MI' from the year's MI' grid. The resulting MID grids are scaled from 2 to −2, although actual values rarely approach either endpoint; a positive value in a grid cell indicates the relative amount of moisture surplus that the cell exhibited for the year of interest when compared to the 100-year mean, while a negative value indicates the relative amount of moisture deficit exhibited by the cell.

To make the MID useful as a drought index, we had to identify meaningful threshold values that distinguish between moisture deficit, i.e., drought, categories. Drought may be viewed as a random phenomenon (Weber and Nkemdirim 1998). Thus, assuming the MID to be a temporally random variable with an approximately normal distribution and a mean

of zero, we selected a set of four threshold values related to the average standard deviation across the 100 annual *MID* grids: *MID* values from 0.5 to <1 standard deviation below the mean, i.e., zero, indicate a mild drought; from 1 to <1.5 standard deviations, a moderate drought; from 1.5 to <2 standard deviations, a severe drought; and values 2 or more standard deviations below the mean indicate extreme drought conditions. Mild, moderate, severe, and extreme wetness may be defined similarly by corresponding standard deviations above the mean, while values between 0.5 and −0.5 standard deviations indicate near normal conditions. To provide additional context regarding our selected thresholds, we created a series of four empirical probability grids by overlaying the annual *MID* grids and subsequently determining, for each grid cell, the proportion of years out of 100 that the cell exhibited: (1) at least a mild drought, (2) at least a moderate drought, (3) at least a severe drought, and (4) an extreme drought.

Historic and Current (2007) Drought Maps Based On Moisture Index Difference—
To illustrate how the *MID* approach depicts significant drought events, we identified 4 years from the latter part of the 20th century during which notable regional droughts had been documented in scientific literature: the Northeastern United States in 1964; the Great Plains region (Central United States) in 1980; the Northwestern United States to the Great Plains in 1988; and the Southwestern United States in 1996 (Andreadis and others 2005, Groisman and Knight 2008, Karl and Quayle 1981, Mueller and others 2005, Namias 1983, Trenberth and Branstator 1992, Trenberth and others 1988). We also examined the *MID* grid for 2007, a year in which the Southeastern United States experienced unusually harsh drought conditions, while a prolonged drought extended into an eighth year in parts of the Western United States (Goodman 2007, Boxall and Powers 2007).

Results and Discussion

100-Year Normal Moisture Index Map—
In addition to serving as the base of reference for our drought analyses, the map of the 100-year mean annual *MI'* for the conterminous United States (fig. 4.1A) may be considered a rough depiction of the country's climatic regimes. Wet climates (*MI'* > 0) are common throughout the Eastern United States, particularly the Northeast, with the wettest (*MI'* >0.5) generally limited to mountainous ecoregion sections or adjacent plateaus, such as sections 211F—Northern Glaciated Allegheny Plateau; 211G—Northern Unglaciated Allegheny Plateau; M211C—Green, Taconic, Berkshire
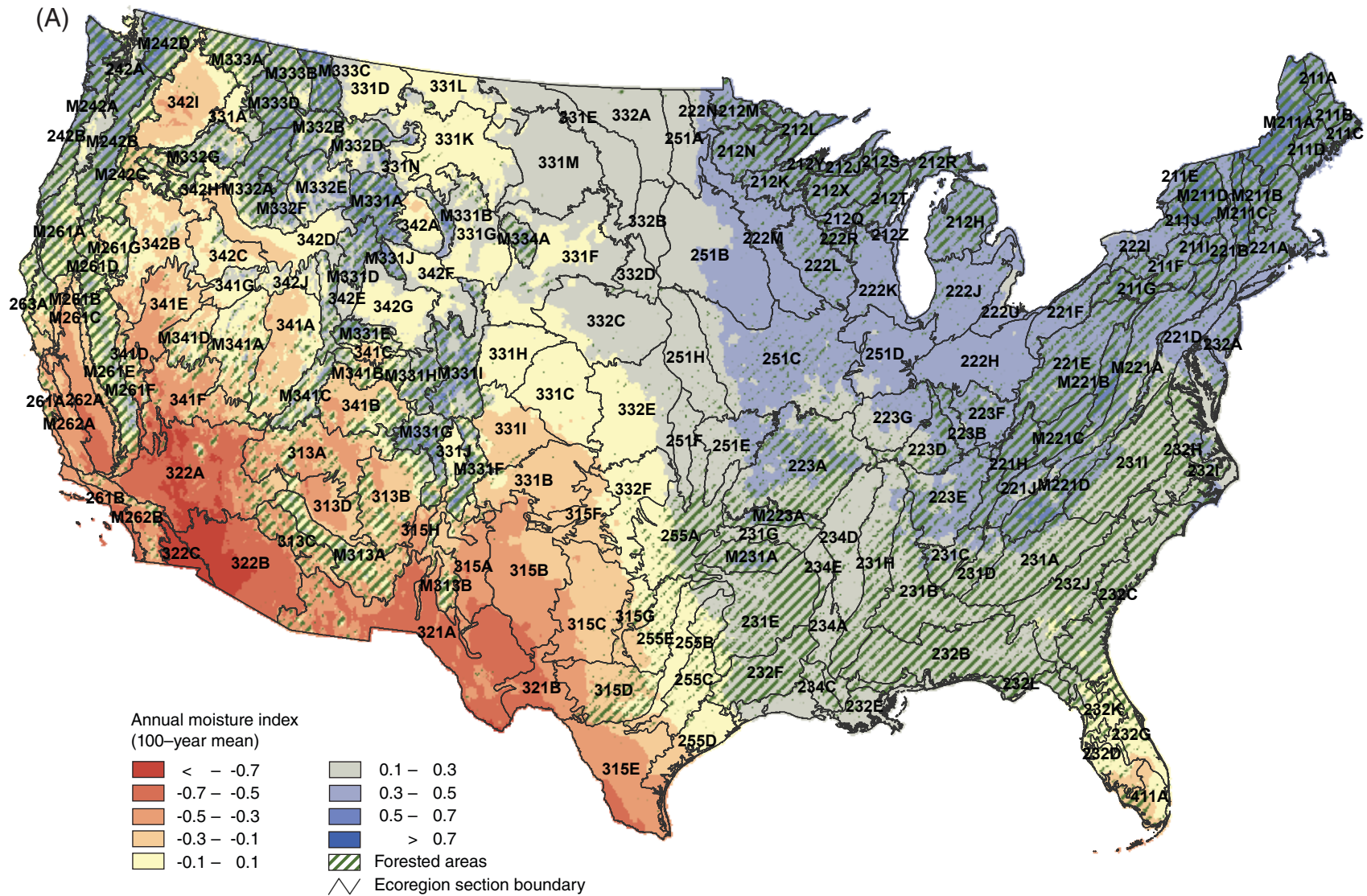
Figure 4.1—The 100-year (1907–2006) (A) mean annual moisture index or MI′, (B) mean annual precipitation, and (C) mean annual potential evapotranspiration for the conterminous United States. Ecoregion section boundaries (Cleland and others 2007) and labels are included for reference. Forest cover data (overlaid green hatching) derived from MODIS imagery by the Forest Service, Remote Sensing Applications Center. (Data source: PRISM Group, Oregon State University) (continued on next page)

(B)

(C)

Precipitation/PET
(mm)

	< 300
	300 – 400
	400 – 550
	550 – 700
	700 – 850
	850 – 1000
	1000 – 1200
	> 1200

Forested areas

Ecoregion section boundary
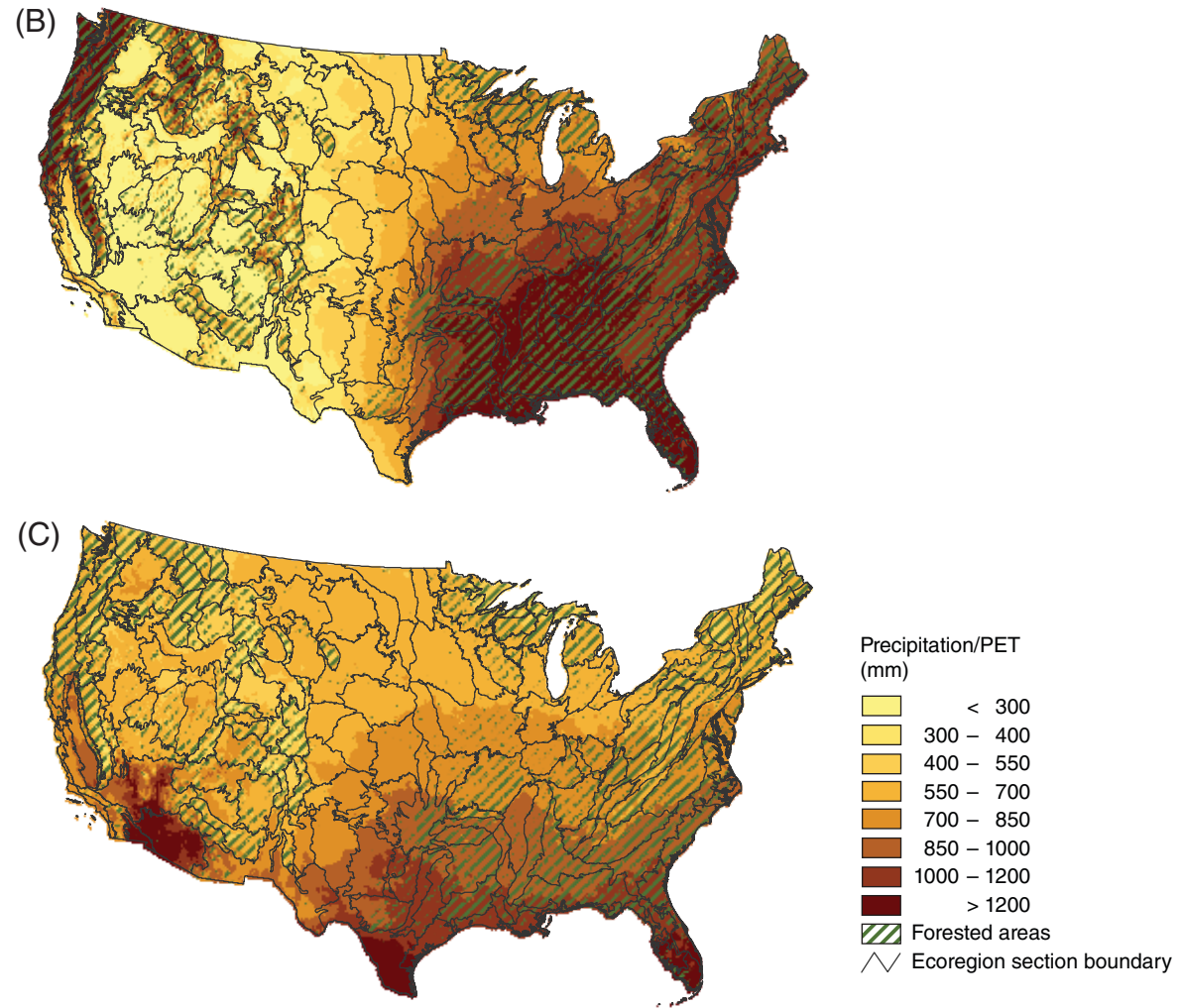
Figure 4.1 (continued)—The 100-year (1907–2006) (B) mean annual precipitation, and (C) mean annual potential evapotranspiration for the conterminous United States. Ecoregion section boundaries (Cleland and others 2007) and labels are included for reference. Forest cover data (overlaid green hatching) derived from MODIS imagery by the Forest Service, Remote Sensing Applications Center. (Data source: PRISM Group, Oregon State University)

Mountains; and M221B—Allegheny Mountains. Perhaps counterintuitively, the driest region of the Eastern United States, in terms of *MI'*, is southern Florida, particularly sections 232D— Florida Coastal Lowlands (Western) and 411A— Everglades in the southwestern portion of the State. This region is not dry in a traditional sense, as it typically receives a large amount of precipitation every year (fig. 4.1B). However, the region's high precipitation level is offset by an also high level of potential evapotranspiration (fig. 4.1C), resulting in negative *MI'* values. Interestingly, the spatial pattern of *MI'* in Florida as depicted in figure 4.1A echoes a recent map of the State's historical drought tendencies during the month of May, the peak of Florida's fire season (Brolley and others 2007).

Dry climates (*MI'* <0) dominate most of the Western United States, where precipitation levels are typically much lower than in the East. Wet climates are generally confined to mountain ranges and adjacent valleys, particularly ecoregion sections in the northern Rocky Mountains and the Pacific Northwest: M242A— Oregon and Washington Coast Ranges, M242B— Western Cascades, M242D—Northern Cascades, M331A—Yellowstone Highlands, and M333C—

Northern Rockies. The driest climates extend across the Southwestern United States, where potential evapotranspiration is consistently high and precipitation is consistently low. Predictably, the lowest *MI'* values (< −0.7) are found across three neighboring ecoregion sections of the Southwest: 322A—Mojave Desert, 322B— Sonoran Desert, and 322C—Colorado Desert.

Drought Category Thresholds—The mean standard deviation of the *MID,* across all grids for the years 1907–2006, was 0.1. The value ranges we subsequently adopted for each drought or wetness category based on this standard deviation are summarized in table 4.1. The approximate theoretical frequencies, i.e., assuming a normal distribution, of *MID* values in each drought category are comparable to the frequencies seen with other commonly used drought indices (table 4.2); nonetheless,

Table 4.1—Moisture index difference value ranges for nine wetness and drought categories, along with the equivalent ranges in standard deviation from the mean value, i.e., zero

Category	Values	Standard deviations
Extreme wetness	≥0.20	≥2.0
Severe wetness	0.15–0.199	1.5–2.0
Moderate wetness	0.10–0.149	1.0–1.5
Mild wetness	0.05–0.099	0.5–1.0
Near normal	0.049– −0.049	0.5– −0.5
Mild drought	−0.05– −0.099	−0.5– −1.0
Moderate drought	−0.10– −0.149	−1.0– −1.5
Severe drought	−0.15– −0.199	−1.5– −2.0
Extreme drought	≤ −0.20	≤ −2.0

Table 4.2—Drought categories, with their corresponding negative value ranges and approximate theoretical frequencies of occurrence, for the moisture index difference and three commonly used drought indices: the Palmer Drought Severity Index, the Standardized Precipitation Index, and the revised Surface-Water Supply Index[a]

Category	MID[b]		PDSI		SPI		Revised SWSI	
	Values	Frequency	Values	Frequency	Values	Frequency	Values	Frequency
		percent		percent		percent		percent
Near normal	0– −0.049	19.10	0– −1.49	23	0– −0.99[c]	34.10	0– −1.99[d]	24
Mild drought	−0.05– −0.099	15	−1.5– −2.99[e]	17				
Moderate drought	−0.10– −0.149	9.20			−1– −1.49	9.20	−2– −2.99	12
Severe drought	−0.15– −0.199	4.40	−3– −3.99	6	−1.5– −1.99	4.40	−3– −3.99	12
Extreme drought	≤ −0.20	2.30	≤ −4	4	≤ −2	2.30	≤ −4	2

MID = moisture index difference, PDSI = Palmer Drought Severity Index, SPI = Standardized Precipitation Index, SWSI = Surface-Water Supply Index.
[a] The PDSI, SPI, and revised SWSI frequencies per category are adapted from previous studies (Garen 1993, Karl 1986, McKee and others 1993, Steinemann 2003).
[b] The MID frequencies assume an approximately normal distribution and a mean of zero.
[c] The SPI is calculated across a series of time scales. According to McKee and others (1993), a drought event for a given time scale represents a period where the SPI is continuously negative and at some point falls below –1. The drought event begins when the SPI first falls below zero, so McKee and others (1993) subsequently labeled the entire value range 0 – –0.99 as mild drought. Steinemann (2003) reinterpreted this range as near normal.
[d] Garen (1993) did not include a mild drought category when reporting frequencies for the modified SWSI, but each one-unit interval of the index represents 12 percent of the theoretical probability of occurrence, e.g., values fall in the range –1 to –2 at a frequency of 12 percent.
[e] Karl (1986) combined mild and moderate drought categories when reporting frequencies for the PDSI.

all of these frequencies should be interpreted cautiously since they depend upon the validity of assumptions about the value distribution and statistical properties of each index (Garen 1993, Steinemann 2003). Although the *MID* is nominally scaled between 2 and −2, actual *MID* values across all grids for the years 1907–2006 were between 0.7 and −0.7, and in most years fell between 0.5 and −0.5.

Drought Probabilities—The drought probability grid maps (fig. 4.2) provide a straightforward assessment of the *MID* due to the empirical manner in which they were constructed, i.e., simply the number of years out of 100 that the annual *MID* was less than or equal to one of the designated threshold values. In general, for all drought categories, the highest drought probabilities are found across the Southern United States (especially the Southwest) as well as the Great Plains region. Nearly the entire conterminous United States displays a moderate probability ($P \geq 0.20$) of at

*Figure 4.2—Probability of (A) at least mild drought, (B) at least moderate drought, (C) at least severe drought, and (D) extreme drought for the conterminous United States. Probabilities were calculated as the number of years out of 100 (years 1907–2006) that the annual moisture index difference (*MID*) was less than or equal to corresponding drought category threshold values, specified in table 4.1. Ecoregion section boundaries (Cleland and others 2007) are included for reference. Forest cover data (overlaid green hatching) derived from MODIS imagery by the Forest Service, Remote Sensing Applications Center. (Data source: PRISM Group, Oregon State University) (continued on next page)*

Probability

☐ 0	☐ 0.15 – 0.2
☐ 0 – 0.01	☐ 0.2 – 0.3
☐ 0.01 – 0.05	☐ 0.3 – 0.4
☐ 0.05 – 0.1	☐ 0.4 – 0.5
☐ 0.1 – 0.15	▨ Forested areas
	∧∨ Ecoregion section boundary
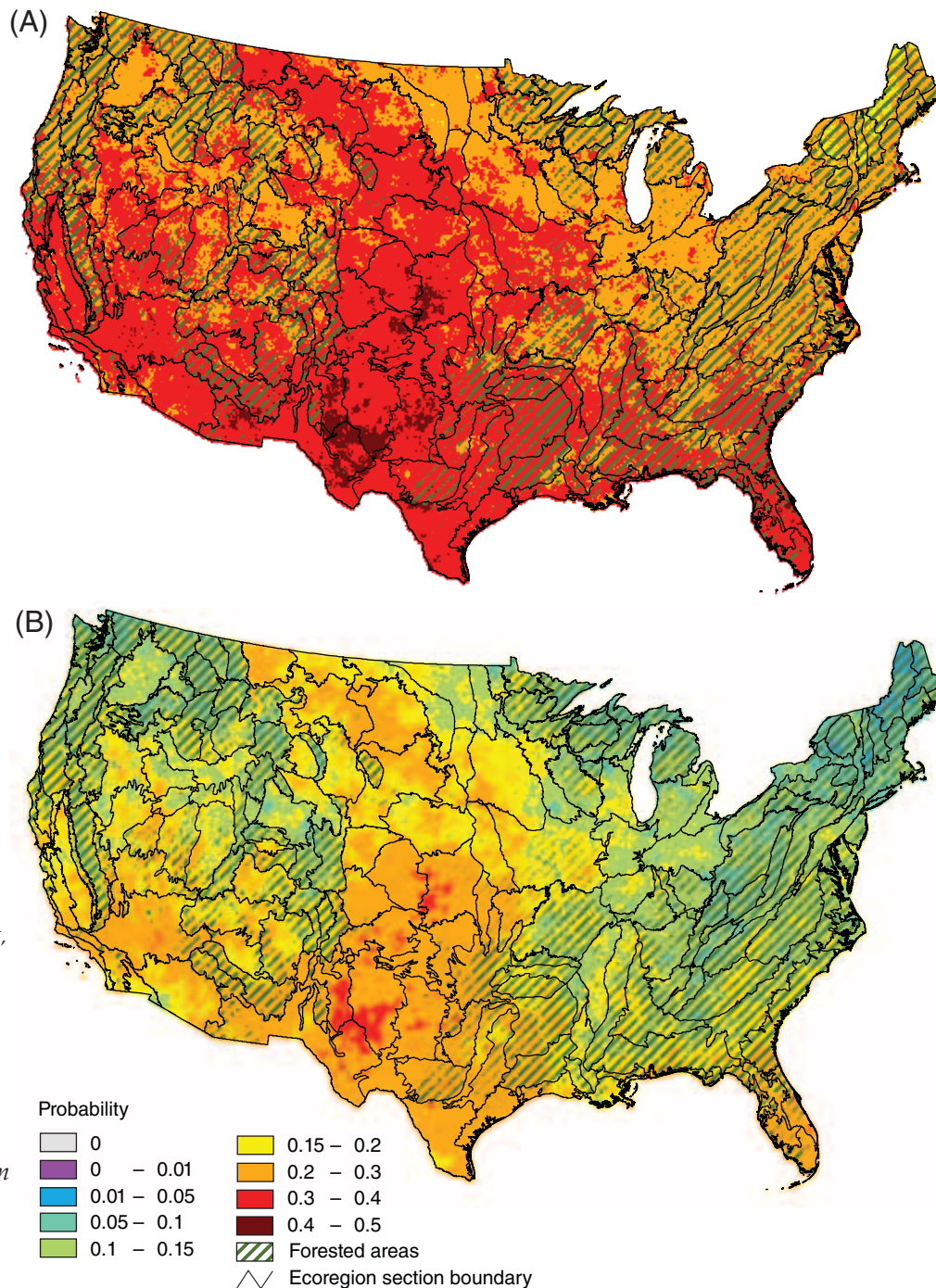
least mild drought conditions, i.e., annual *MID* values < −0.05, occurring in any given year, with the exception of patches in a few ecoregion sections of the Northeast: most notably M211A—White Mountains; M211B—New England Piedmont; M211C—Green, Taconic, Berkshire Mountains; and M211D—Adirondack Highlands (fig. 4.2A). On the other hand, most of the country exhibits a low probability (*P* <0.05) that extreme drought conditions will occur in a given year (fig. 4.2D). Indeed, some areas show a zero probability (P = 0) of extreme drought, although this likely reflects the limited precision of probabilities estimated using 100 years of available data. Probabilities of extreme drought are somewhat higher (0.05 ≤ *P* < 0.10) in the northern Great Plains region and along the gulf coast, but the highest probabilities of extreme drought are patchily distributed throughout the Southwestern United States and the southern Great Plains region. Taking into consideration the probability grids for all four drought categories, these latter two regions appear to represent the most drought-

Figure 4.2 (continued)—Probability of (C) at least severe drought, and (D) extreme drought for the conterminous United States. Probabilities were calculated as the number of years out of 100 (years 1907–2006) that the annual moisture index difference (MID) was less than or equal to corresponding drought category threshold values, specified in table 4.1. Ecoregion section boundaries (Cleland and others 2007) are included for reference. Forest cover data (overlaid green hatching) derived from MODIS imagery by the Forest Service, Remote Sensing Applications Center. (Data source: PRISM Group, Oregon State University)

(C)

(D)

Probability

☐ 0	☐ 0.15 − 0.2
☐ 0 − 0.01	☐ 0.2 − 0.3
☐ 0.01 − 0.05	☐ 0.3 − 0.4
☐ 0.05 − 0.1	☐ 0.4 − 0.5
☐ 0.1 − 0.15	▨ Forested areas
	⋀⋁ Ecoregion section boundary
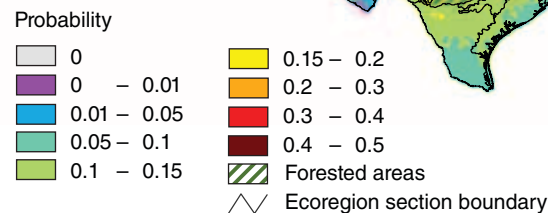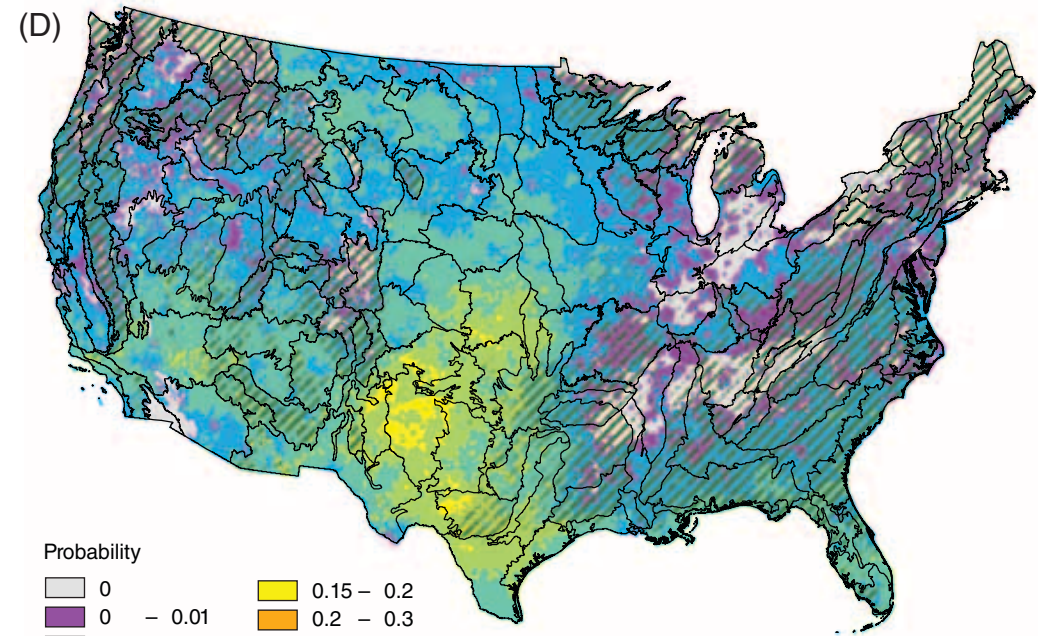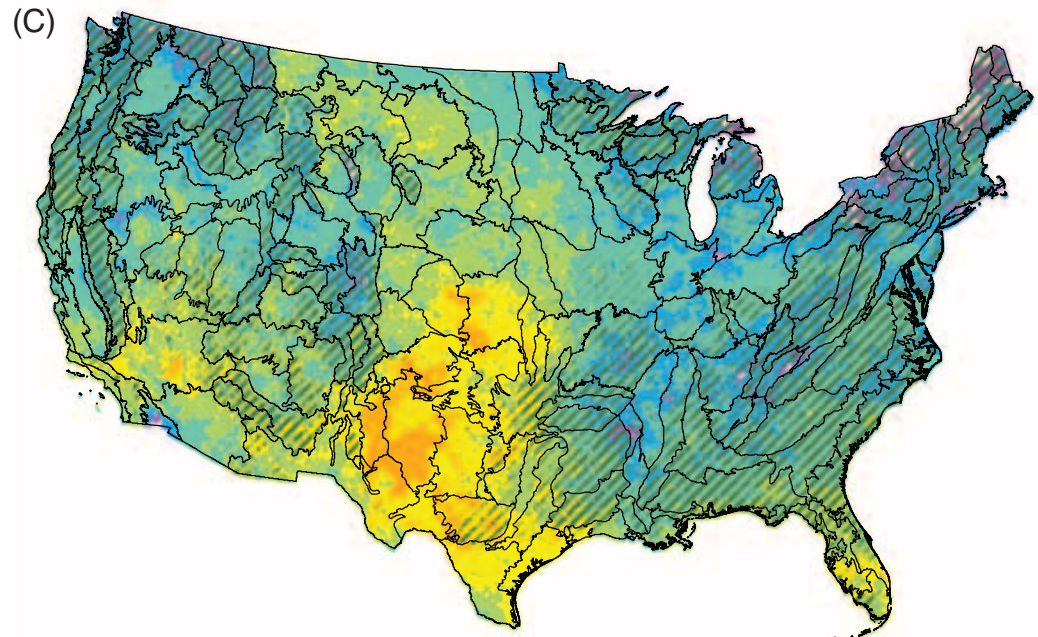
prone areas in the conterminous United States according to our analytical approach. While both regions tend to be dry climatically, they also exhibit a reasonably wide range of 100-year mean MI' values, i.e., they have somewhat varied climatic regimes through time. It is further worth noting that the most affected ecoregion sections are largely unforested.

Historic Drought Maps—The *MID* approach yields effective 1-year snapshots of drought conditions, as demonstrated by its ability to capture several significant drought events from recent decades. For example, the Northeastern United States was subjected to a drought between 1962 and 1965 due to cyclonic activity off the Atlantic coast, likely caused by colder-than-normal sea surface temperatures, which led to wind anomalies and less moisture on land in New England and the Mid-Atlantic region (Namias 1983). The *MID* map for 1964 (fig. 4.3A) subsequently shows a large area of severe-to-extreme drought covering most of the Northeast. The *MID* map for 1980 (fig.

Figure 4.3—Moisture index difference (MID) maps for 4 years in which notable regional droughts occurred: (A) Northeastern United States, 1964; (B) Great Plains, 1980; (C) Northwestern United States and Great Plains, 1988; and (D) Southwestern United States, 1996. Ecoregion section boundaries (Cleland and others 2007) are included for reference. Forest cover data (overlaid green hatching) derived from MODIS imagery by the Forest Service, Remote Sensing Applications Center. (Data source: PRISM Group, Oregon State University) (continued on next page)

(A)

(B)

Moisture index difference

≤ -0.20	(Extreme deficit)
-0.199 – -0.15	(Severe deficit)
-0.149 – -0.10	(Moderate deficit)
-0.099 – -0.05	(Mild deficit)
-0.049 – 0.049	(Near normal)
≥ 0.05	(Surplus)
Forested areas	
Ecoregion section boundary	
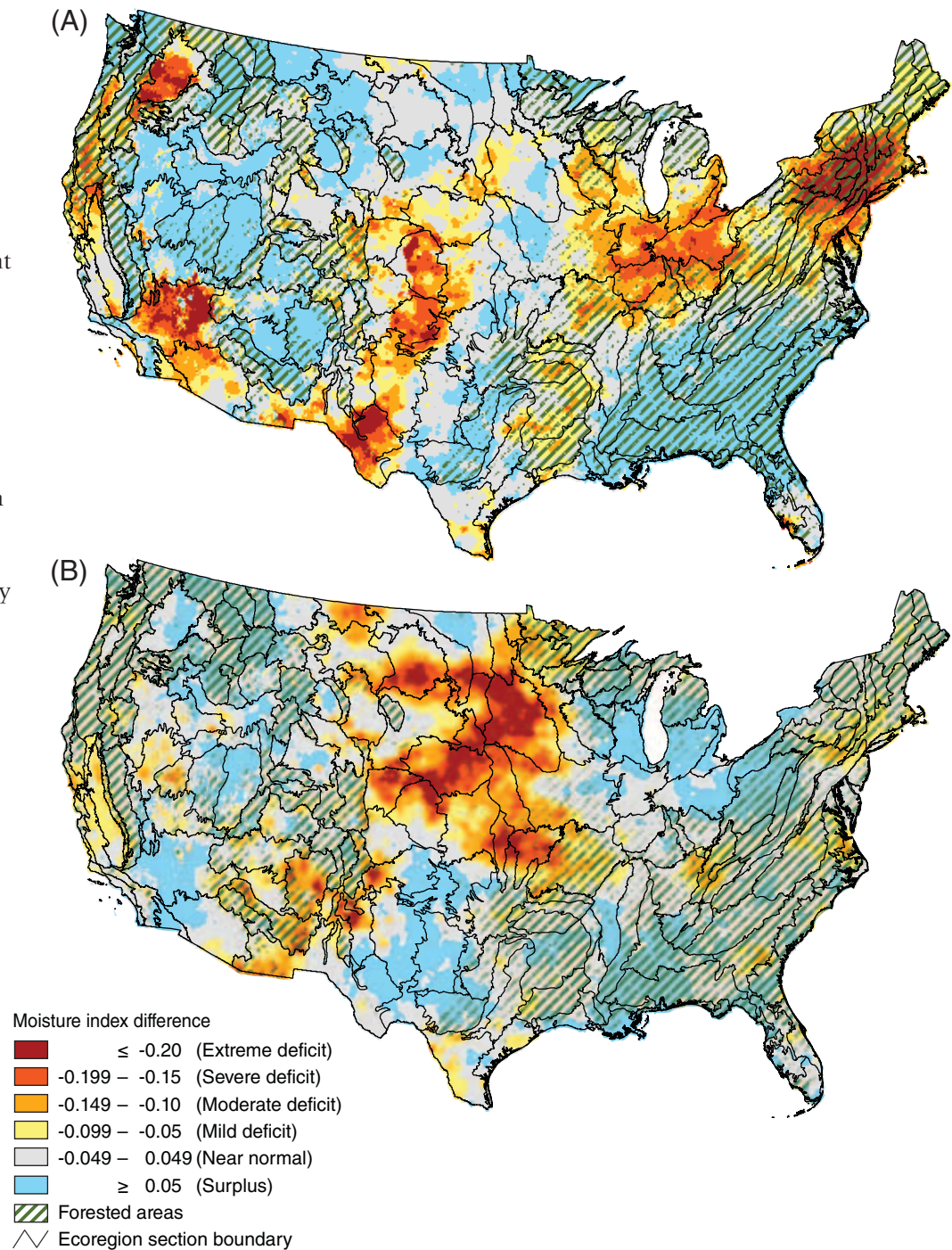
4.3B) shows an area of severe-to-extreme drought centered over the northern Great Plains region. While a summer heat wave eventually impacted much of the country that year, drought conditions persisted across the northern Great Plains for several months in a row (Karl and Quayle 1981). A drought that extended across much of the United States in 1988 was reported, shortly after its occurrence, as the most expensive natural disaster in the country's history (Trenberth and Branstator 1992). As illustrated by the *MID* map for 1988 (fig. 4.3C), the northern Great Plains region, southern Texas, the Northwestern United States, and the west coast were particularly affected (Andreadis and others 2005, Trenberth and others 1988). More recently, drought has deleteriously impacted vegetation in the Southwestern United States. Drought conditions occurred in 6 out of 10 years between 1995 and 2004 in this region, and extreme drought was widespread in 1996 (fig. 4.3D), precipitating extensive mortality

Figure 4.3 (continued)—Moisture index difference (MID) maps for 4 years in which notable regional droughts occurred: (C) Northwestern United States and Great Plains, 1988; and (D) Southwestern United States, 1996. Ecoregion section boundaries (Cleland and others 2007) are included for reference. Forest cover data (overlaid green hatching) derived from MODIS imagery by the Forest Service, Remote Sensing Applications Center. (Data source: PRISM Group, Oregon State University)

Moisture index difference

⬛ (dark red)	≤ -0.20 (Extreme deficit)
⬛ (orange-red)	-0.199 – -0.15 (Severe deficit)
⬛ (orange)	-0.149 – -0.10 (Moderate deficit)
⬛ (yellow)	-0.099 – -0.05 (Mild deficit)
⬛ (gray)	-0.049 – 0.049 (Near normal)
⬛ (blue)	≥ 0.05 (Surplus)
▨	Forested areas
∧∨	Ecoregion section boundary
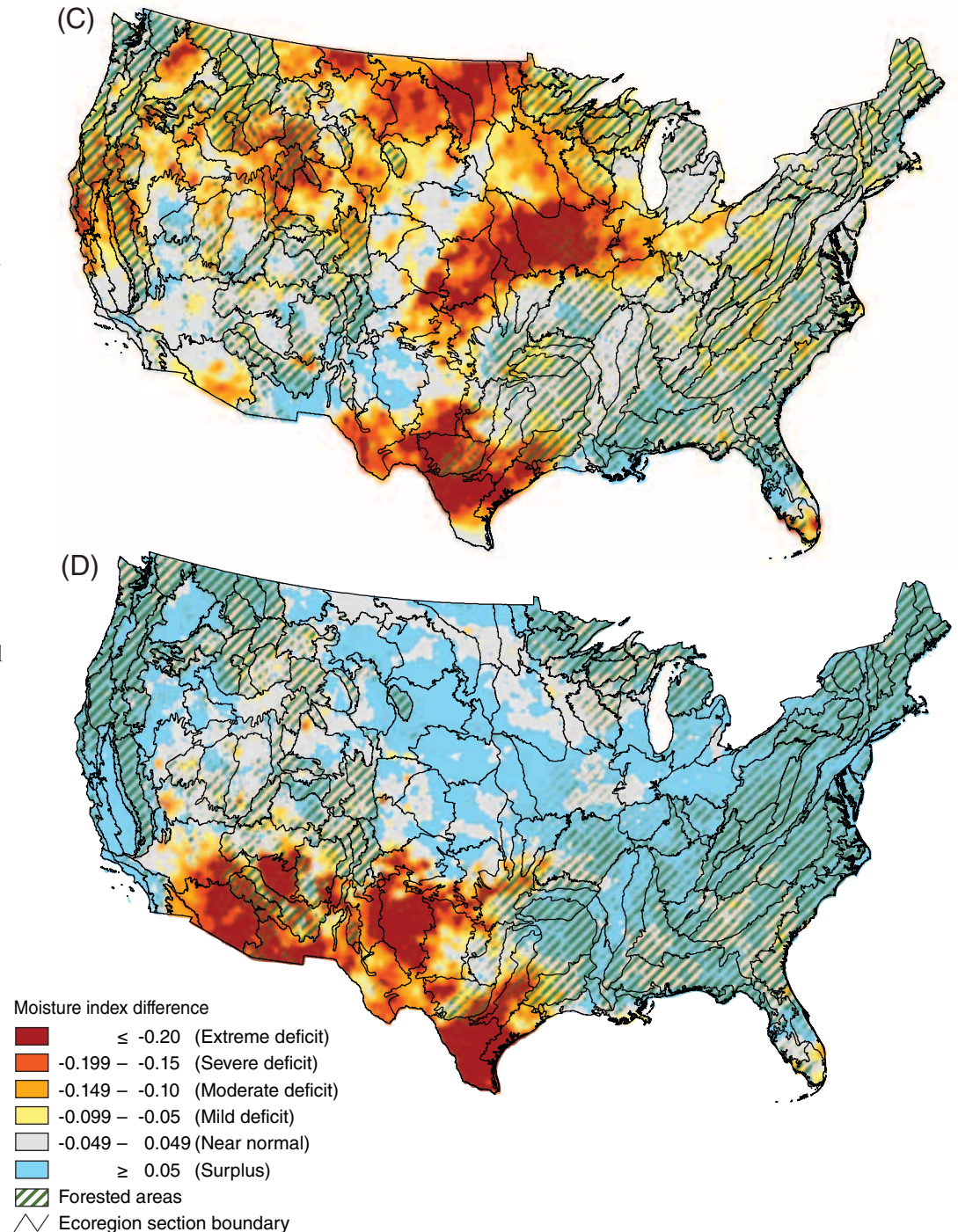
in pinyon-juniper woodlands (Mueller and others 2005). Actually, since drought conditions persisted for so long in the Southwest, a multiyear analysis could be quite informative with respect to the observed mortality patterns; this suggests a potentially fruitful area of future work with the *MID* approach.

Current (2007) Drought Map—The *MID* map for 2007 is shown in figure 4.4. In 2007, much of the Southeastern United States reached exceptional drought levels for the first time in more than 100 years, leading government officials in several States and municipalities to implement strict water restrictions (Goodman 2007). In the *MID* map, severe to extreme drought conditions covered large percentages of land area in several heavily forested ecoregion sections: 221J—Central Ridge and Valley, 223E—Interior Low Plateau-Highland Rim, 231A—Southern Appalachian Piedmont, 231B—Coastal Plains-Middle, 231C—Southern Cumberland Plateau, 231D—Southern Ridge and Valley, 231I—Central Appalachian Piedmont, 232C—Atlantic Coastal Flatwoods, and 232I—Northern Atlantic Coastal Flatwoods. Pockets of severe-to-

extreme drought were distributed across other sections in the Southeast. The *MID* map also shows extreme drought in southern Florida, especially in portions of sections 232D—Florida Coastal Lowlands-Gulf and 411A—Everglades. Lake Okeechobee, which is located in the extreme northern portion of 411A, fell to a record low in 2007, such that 12,000 acres of the lakebed were actually burned by wildfire in May of that year (O'Driscoll 2007).

Moderate-to-extreme drought covered most of central to southern California in 2007. Extreme drought also appeared in parts of the Intermountain West, at times reaching into forested portions of sections such as M313A—White Mountains-San Francisco Peaks, M331E—Uinta Mountains, and M341A—East Great Basin and Mountains. Notably, the *MID* grid for 2007 depicts normal to surplus conditions across much of the Central United States, particularly the southern Great Plains region; this was a major departure from the previous 2 years for this area, where drought conditions contributed to high wildfire incidence (O'Driscoll 2007).
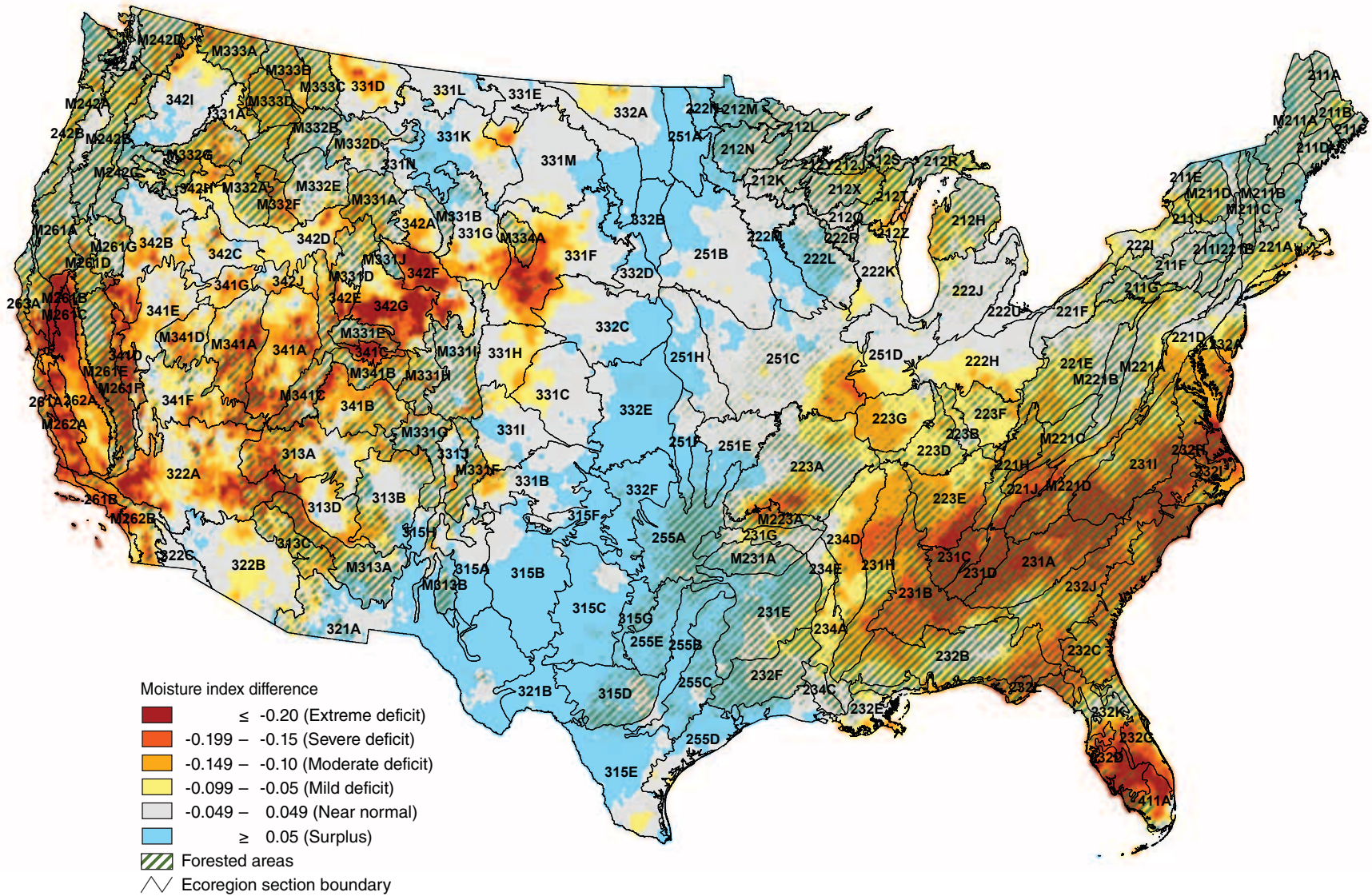
Figure 4.4—*Map of the 2007 moisture index difference (*MID*) for the conterminous United States. Ecoregion section boundaries (Cleland and others 2007) and labels are included for reference. Forest cover data (overlaid green hatching) derived from MODIS imagery by the Forest Service, Remote Sensing Applications Center. (Data source: PRISM Group, Oregon State University)*

Issues and Implications—In this chapter, we presented a methodology for characterizing drought on an annual time step and further applied the approach to estimate probabilities of different levels of drought severity for the conterminous United States. The *MID* approach is computationally simple and repeatable, requiring only climate variables and omitting soil or other environmental factors that are unavailable nationally at fine scales. Nevertheless, because the *MID* only accounts for part of the entire environmental moisture balance, it is does not replace other drought indicators such as the PDSI or the many indices applied to hydrological or agricultural drought. Indeed, no drought monitoring tool is applicable for all analyses, especially since drought may be defined differently depending on whether the analyst is focused on moisture supply, moisture demand, or the socioeconomic consequences of a drought event (Brown and others 2008, Weber and Nkemdirim 1998). We must also acknowledge that our annual time window is arbitrary; drought events may last longer than a year, or even if < 12 months in duration, may start in the latter part of 1 year and continue into the next. The *MID* approach can be adapted for any period of consecutive months, although this complicates the calculation of a corresponding "normal" *MI* to subtract from the *MI* for the time period of interest. Other high-resolution approaches to monitoring drought are currently in development. For example, the Vegetation Drought Response Index (VegDRI) combines traditional drought indices (PDSI and SPI) with remote-sensing-derived vegetation indices and other environmental data to map vegetative drought stress in close to real-time at a 1-km^2 spatial resolution; although it is currently at a regional pilot stage, there are plans to eventually expand the coverage of VegDRI to a national scale (Brown and others 2008). For monitoring of current drought conditions, this method or something similar may ultimately be a preferred alternative to our proposed *MID* approach. In the meantime, data generated using our approach may be useful as a high-resolution complement to other drought mapping products, e.g., Drought Monitor GIS data. Moreover, one noteworthy potential application of the *MID* approach is the generation of explanatory variables in predictive models pertaining to forest health issues, particularly if those models are intended to incorporate multiple decades of historical drought data. For instance, *MID* datasets could be employed in broad-scale risk analyses for forest pests that utilize drought-stressed trees or otherwise exhibit increased activity during drought conditions.

Literature Cited

Akin, W.E. 1991. Global patterns: climate, vegetation, and soils. Norman, OK: University of Oklahoma Press. 370 p.

Alley, W.M. 1984. The Palmer Drought Severity Index: limitations and assumptions. Journal of Climate and Applied Meteorology. 23: 1100–1109.

Andreadis, K.M.; Clark, E.A.; Wood, A.W. [and others]. 2005. Twentieth-century drought in the conterminous United States. Journal of Hydrometeorology. 6: 985–1001.

Boxall, B.; Powers, A. 2007. The Nation; Colorado River water deal is reached; the Interior Secretary calls it an 'agreement to share adversity'. Los Angeles, CA: Los Angeles Times. December 14: 16.

Brolley, J.M.; O'Brien, J.J.; Schoof, J.; Zierden, D. 2007. Experimental drought threat forecast for Florida. Agricultural and Forest Meteorology. 145: 84–96.

Brown, J.A.; Wardlow, B.D.; Tadesse, T. [and others]. 2008. The Vegetation Drought Response Index (VegDRI): a new integrated approach for monitoring drought stress in vegetation. GIScience & Remote Sensing. 45(1): 16–46.

Clark, J.S. 1989. Effects of long-term water balances on fire regime, north-western Minnesota. Journal of Ecology. 77: 989–1004.

Cleland, D.T.; Freeouf, J.A.; Keys, J.E. [and others]. 2007. Ecological subregions: sections and subsections for the conterminous United States. (A.M. Sloan, technical editor). Gen. Tech. Rep. WO-76. Washington, DC: U.S. Department of Agriculture Forest Service. [Map, presentation scale 1: 3,500,000; colored]. [Also on CD–ROM as a Geographic Information System coverage in ArcINFO format].

Daly, C.; Gibson, W.P.; Taylor, G.H. [and others]. 2002. A knowledge-based approach to the statistical mapping of climate. Climate Research. 22: 99–113.

Garen, D.C. 1993. Revised surface-water supply index for Western United States. Journal of Water Resources Planning and Management. 119(4): 437–454.

Goodman, B. 2007. Drought-stricken South facing tough choices. New York: New York Times. October 16: 14.

Groisman, P.Y.; Knight, R.W. 2008. Prolonged dry episodes over the conterminous United States: new tendencies emerging during the last 40 years. Journal of Climate. 21: 1850–1862.

Guttman, N.B. 1998. Comparing the Palmer Drought Index and the Standardized Precipitation Index. Journal of the American Water Resources Association. 34(1): 113–121.

Heim, R.R. 2002. A review of twentieth-century drought indices used in the United States. Bulletin of the American Meteorological Society. 83(8): 1149–1165.

Kareiva, P.M.; Kingsolver, J.G.; Huey, B.B., eds. 1993. Biotic interactions and global change. Sunderland, MA: Sinauer Associates, Inc. 559 p.

Karl, T.R. 1986. The sensitivity of the Palmer Drought Severity Index and Palmer's Z-Index to their calibration coefficients including potential evapotranspiration. Journal of Climate and Applied Meteorology. 25: 77–86.

Karl, T.R.; Quayle, R.G. 1981. The 1980 summer heat wave and drought in historical perspective. Monthly Weather Review. 109(10): 2055–2073.

Keetch, J.J.; Byram, G.M. 1968. A drought index for forest fire control. Res. Pap. SE–38. Asheville, NC: U.S. Department of Agriculture Forest Service, Southeastern Forest Experiment Station. 33 p.

Keyantash, J.; Dracup, J.A. 2002. The quantification of drought: an evaluation of drought indices. Bulletin of the American Meteorological Society. 83(8): 1167–1180.

Mattson, W.J.; Haack, R.A. 1987. The role of drought in outbreaks of plant-eating insects. BioScience. 37(2): 110–118.

McKee, T.B.; Doesken, N.J.; Kleist, J. 1993. The relationship of drought frequency and duration to time scales. In: Eighth conference on applied climatology. American Meteorological Society: 179–184.

Mueller, R.C.; Scudder, C.M.; Porter, M.E. [and others]. 2005. Differential tree mortality in response to severe drought: evidence for long-term vegetation shifts. Journal of Ecology. 93: 1085–1093.

Namias, J. 1983. Some causes of United States drought. Journal of Climate and Applied Meteorology. 22: 30–39.

National Climatic Data Center. 2007. Time bias corrected divisional temperature-precipitation-drought index. Documentation for dataset TD–9640. http://www1.ncdc. noaa.gov/pub/data/cirs/drought.README. [Date accessed: May 9, 2008].

National Drought Mitigation Center. 2008. U.S. Drought Monitor GIS data archive. http://drought.unl.edu/dm/ dmshps_archive.htm. [Date accessed: May 9].

O'Driscoll, P. 2007. A drought for the ages; from the dried lake beds of Florida to the struggling ranches of California, a historic lack of rain is changing how Americans live. McLean, VA: USA Today. June 8: 1A.

PRISM Group. 2008. 2.5-arcmin (4 km) gridded monthly climate data. ftp://prism.oregonstate.edu//pub/prism/us/ grids. [Date accessed: March 1].

Schoennagel, T.; Veblen, T.T.; Romme, W.H. 2004. The interaction of fire, fuels, and climate across Rocky Mountain forests. BioScience. 54(7): 661–676.

Smith, G.; Coulston, J.; Jepsen, E.; Pritchard, T. 2003. A national ozone biomonitoring program - results from field surveys of ozone sensitive plants in northeastern forests (1994-2000). Environmental Monitoring and Assessment. 87: 271–291.

Steinemann, A. 2003. Drought indicators and triggers: a stochastic approach to evaluation. Journal of the American Water Resources Association. 39(5): 1217–1233.

Svoboda, M.; LeComte, D.; Hayes, M. [and others]. 2002. The Drought Monitor. Bulletin of the American Meteorological Society. 83(8): 1181–1190.

Thornthwaite, C.W. 1948. An approach towards a rational classification of climate. Geographical Review. 38(1): 55–94.

Trenberth, K.E.; Branstator, G.W. 1992. Issues in establishing causes of the 1988 drought over North America. Journal of Climate. 5: 159–172.

Trenberth, K.E.; Branstator, G.W.; Arkin, P.A. 1988. Origins of the 1988 drought. Science. 242(4886): 1640–1645.

Weber, L.; Nkemdirim, L. 1998. Palmer's drought indices revisited. Geografiska Annaler. Series A, Physical Geography. 80(2): 153–172.

Willmott, C.J.; Feddema, J.J. 1992. A more rational climatic moisture index. Professional Geographer. 44(1): 84–87.